ESRF	**Experiment title:** Phase-enhanced x-ray microtomography for the study of comparative head anatomy in insects	**Experiment number**: ME 1231
Beamline: ID19	**Date of experiment**: from: 25 Oct 2005 to: 28 Oct 2005	**Date of report**: 25 Aug 2005 *Received at ESRF:*
Shifts: 6	**Local contact(s)**: Dr. Peter Cloetens	

Names and affiliations of applicants (* indicates experimentalists):

Oliver BETZ (University of Tübingen), Ulrike G.K. WEGST (Max-Planck-Institut für Metallforschung, Stuttgart), Daniela WEIDE (University of Tübingen)

Report:

Part 1 (O. Betz, D. Weide): Head morphology of staphylinid beetles.

Generally, staphylinid beetles (Coleoptera: Staphylinidae) are known as predators. However, in several groups, the feeding mechanism has changed, and especially some members of the subfamily Aleocharinae are known as feeders of fungal spores. Our studies focus on the changes in the head anatomy, which have occurred in correlation with this novel feeding strategy. During the experiments we obtained 43 µCTs of the following representatives of Staphylinidae: *Aleochara ripicola*, *Atheta laticollis*, *Autalia impressa*, *Eumicrota* sp., *Gyrophaena boleti*, *G. fasciata*, *Gyrophaena* sp., *Homalota* sp., *Oligota parva*, *Oxypoda alternans*, *Pagla* sp., *Polylobus* sp., and *Stictalia* sp., all of them being members of the subfamily Aleocharinae. For comparative purposes, sporophagous as well as non-sporophagous taxa were considered. As outgroups we also included representatives of the subfamilies Tachyporinae (*Tachinus* cf. *humeralis*, *Tachyporus* sp., *Tachyporus nitidulus*, *Tachyporus chrysomelinus*), Habrocerinae (*Habrocerus capillaricornis*), Oxytelinae (e. g., *Oxytelus sculpturatus*), and the plesiomorphic Omaliinae (*Lesteva longelytrata*, *Omalium rivulare*) and Proteininae (*Proteinus brachypterus*). The smaller samples were investigated in a filed of view that amounted to 0.60 mm side length, leading to a spatial resolution of 0.29 µm. For the bigger samples we changed the optics, so we received a 1.43 mm field of view resulting in a spatial resolution of 0.70 µm. The camera distance always amounted to 10 mm. With these data we are able to comparatively analyse the origins and insertions of the head muscles and, for the first time, to render the 3D appearance of internal head structures such as the tentorium (= inner head skeleton). This will be a major step in understanding the evolution of the head anatomy in a major group of beetles.

Hitherto, we have analysed the data sets of four species (*A. laticollis*, *G. fasciata*, *O. rivulare*, *T. chrysomelinus*) and compared the results with known data of the families Hydraenidae, Spercheidae and Helophoridae. Compared with these outgroups there are few changes apparent in antennal, mandibular, and labial muscles. Some modifications also occur in muscles, which move the labrum, i.e. one of both the labral movers (Musculus frontolabralis and M. frontoepipharyngealis) might be reduced. It is also conspicuous that one muscle that is associated with the hypopharynx could only be found in one of the four species under investigation, whereas it is always present in the members of the outgroups.

The structure of the tentorium is similar within the different species. Its main components are the corpotentorium with anterior, dorsal, and posterior arms. The tentorium can be compact like in *O. rivulare*, whereas it is more delicate in other species (e.g., *A. laticollis* and *G. fasciata*). Moreover, in some inner skeletons (e.g. tentorium of *Tachyporus nitidulus*) there is no compact corpotentorium or some components like the dorsal arm can be reduced. Figure 1a shows the results for one species using the 3D segmentation tool of the software amira® for rendering the 3D structure of the inner head skeleton.

Beside the tentorium, other sclerites ensure the stability of the head capsule and serve as attachment structure for a number of head muscles. Additionally, based on their position one can assume that the sclerites, which are located on the dorsal wall of the hypopharynx (see Fig. 1a, blue), give stability to the hypopharynx.

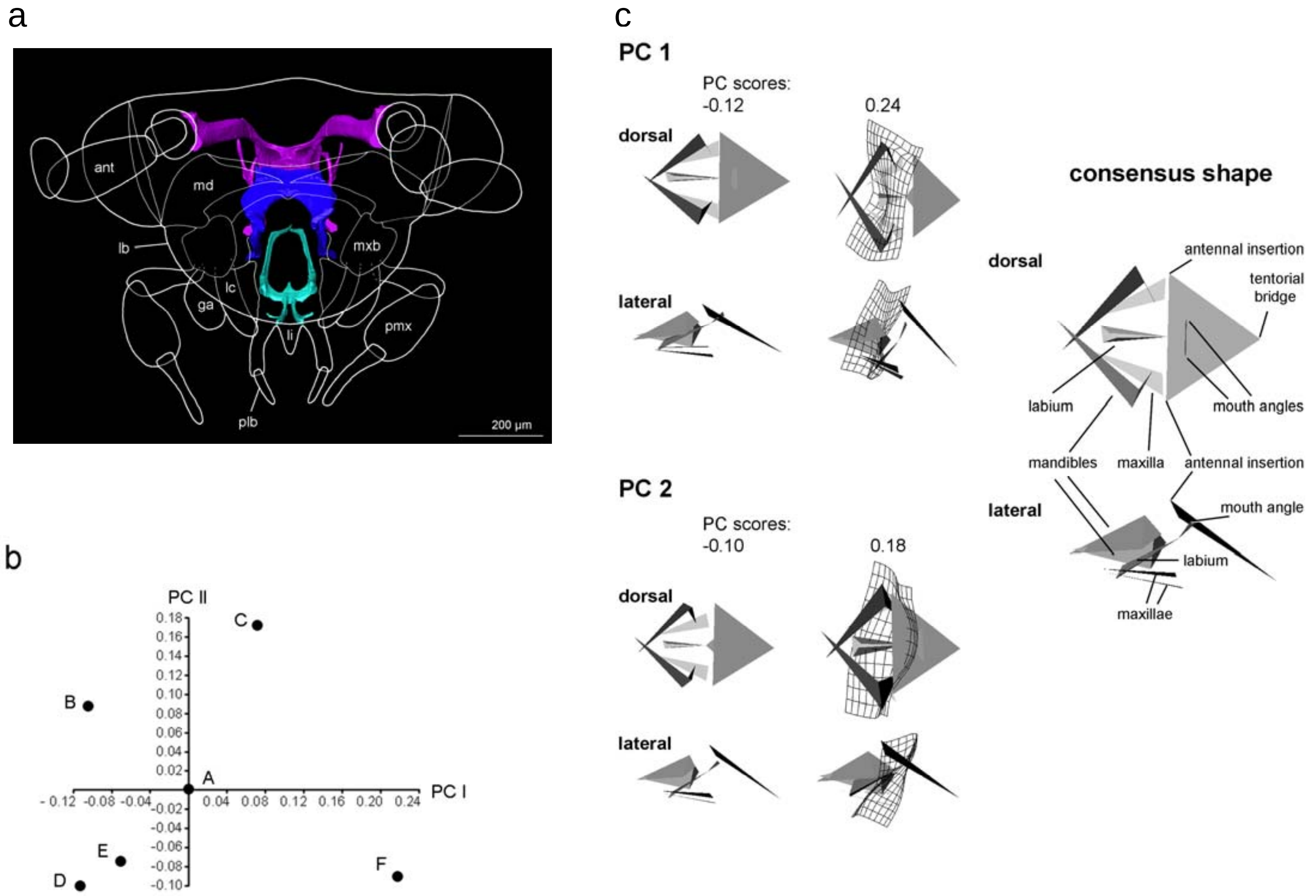

Fig. 1: **(a)** *Gyrophaena fasciata*. Combination of a hand drawn sketch of the head capsule (fronto-dorsal aspect) with the 3D reconstruction of the sclerites of the hypopharyngeal (green) and prementum (blue) region, and the tentorium (purple). Reconstruction by means of amira®. Abbreviations: ant = antenna, ga = galea, lb = labrum, lc = lacinia, li = ligula, md = mandible, mxb = maxillary base, plb= labial palpus, pmx = maxillary palpus. **(b)** Shape variation among the heads of four staphylinid species as visualized by PCA. The scatter diagram shows the dispersion of the investigated specimens along the first two axes of PCA. A Consensus form, B *Omalium rivulare*, C *Tachyporus chrysomelinus*, D *Gyrophaena fasciata* (specimen 1), E *G. fasciata* (specimen 2), F *Atheta laticollis*. **(c)** Dorsal and latero-ventral aspects of shape variation represented by the first two principal components (PC1 and PC 2) as visualized by transformation grids showing the shape differences from the negative (reference shapes) to the positive (target shapes) extremes of the principal components (cf. principal components scatter diagram in Fig.b). On the right side, there is displayed the consensus shape (i.e., both PC1 and PC2 scores are set to zero) with explanations of the parts of the head as represented by the selected landmarks. The transformation grids are drawn in regions, where the shape differences are most obvious.

In order to quantify the anatomical differences between the different species, we apply the techniques of 3D geometric morphometrics to our µCT data. Twenty-six easily identifiable homologous landmarks were used, most of them describing the insertion points of head muscles, which move the different head appendages such as the mouthparts and the antennae. The landmarks were set within selected 2D images of the Synchrotron µCT voxel datasets with the coordinate measurement tool of VGStudio Max. The 3D coordinates of each landmark were stored within an Excel datasheet, which could be directly read into Morphologika (O`Higgins & Jones 2004), in which all the following analyses were performed. For illustration purposes, a first example of these analyses as performed in four species is shown in Fig.1b-c. Our

ESRF data will make it possible to extend these analyses to all of the more than 20 investigated species in order to find quantitative correlations between their morphology, their systematic position, and their feeding type.

In addition to the regular experiments we did a short study with samples that were fixated with osmium tetroxide. This aimed at analysing whether osmium “staining” enhances contrast of soft tissue. For this propose we used individuals, which were scanned at an energy close to the absorption maximum of osmium (20 KeV). Our results indicate that the fixation with osmium tetroxide is indeed useful to enhance the contrast of soft tissue (Fig.2).

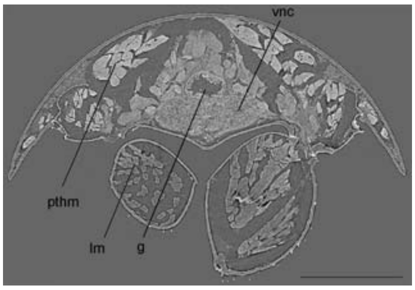

Fig. 2: *Tachyporus* sp. (Coleoptera, Staphylinidae). Virtual transversal section through the prothorax obtained by Synchrotron µCT to show the effect of osmium "staining". The beam energy was set to 20 keV. The beetle was cut posterior to its prothorax, so that osmium tetroxide had easy access to the muscles, the gut, and the ventral nerve chord, which are located in the prothorax. As a result, this tissue appears brighter in the beam than the leg muscles, which were entirely enclosed within the cuticular leg-capsule and thus less accessible to the osmation. Abbreviations: g gut, lm muscles of the leg, pthm muscles of the prothorax, vnc ventral nerve chord. Bar = 300 µm.

Part 2 (M. Heethoff, O. Betz): Some preliminary µCT studies were conducted with whole microarthropods. We used specimens of the parthenogenetic oribatid mite *Archegozetes longisetosus* Aoki (Acari, Oribatida). It was aimed to test fixation methods of intact animals having a strongly sclerotized cuticle for subsequent phase enhanced µCT analyses. Data were obtained with a spatial resolution of 0.7 µm and analyzed with the volume graphics software VGStudio Max (Volume Graphics). Cuticular structures, muscles and tissues of the digestive system were obtainable in detail (Fig.3), less dense tissues such as the synganglion and the ovary had a large signal-overlap with the surrounding air. These were obtained on the virtual sections but got lost in 3D renditions. Based on these results, a new proposal for beamtime on ID19 was submitted and approved (Heethoff, Betz). Methods enhancing the detection of soft tissues such as holotomography will be tested as well as the analysis of unfixed fresh material (eggs).

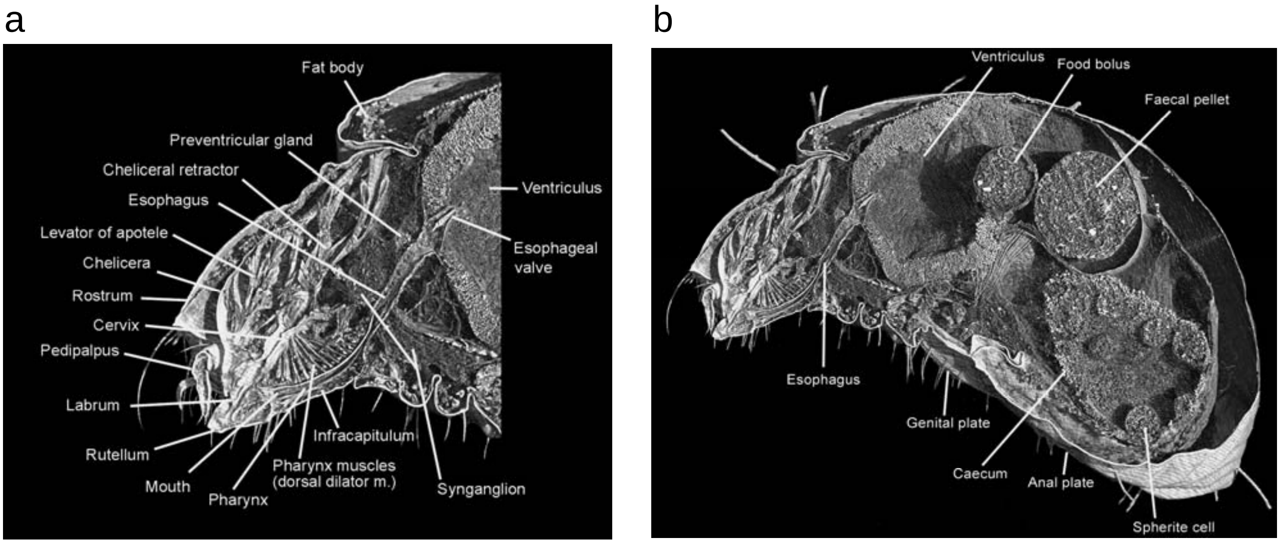

Fig.3: **(a)** Sagittal 3D rendition of the head region of *Archegozetes longisetosus*. Note that the synganglion is visible but no detailed structures can be observed. (b) Sagittal 3D rendition through the whole animal. Spherite cells of the caecum can be seen as well as processed food. The length of the animal in (b): 0.5 mm.

Hitherto, there are 2 publications in preparation or already in press, in which results of our experiments will be incorporated:

Betz, O., Wegst, U., Weide, D., Heethoff, M., Helfen, L., Lee, W.-K., Breidenbach, B., Mecke, K., Sheppard, A., Cloetens, P. (in prep.): Imaging applications of Synchrotron X-ray micro-tomography in biological morphology and biomaterial science

Heethoff, M., Laumann, M. & Bergmann. P. (in press). Adding to the reproductive biology of the parthenogenetic oribatid mite *Archegozetes longisetosus* (Acari, Oribatida, Trhypochthoniidae), Turk. J. Zoology

Literature:

O`Higgins, P. & Jones, N. (2004). Morphologika: tools for shape analysis, Version 2.0. University College London.